

Probing the physical conditions of dense molecular gas in (U)LIRGs with LVG modeling

Ioanna Leonidaki (ISAARS-NOA)

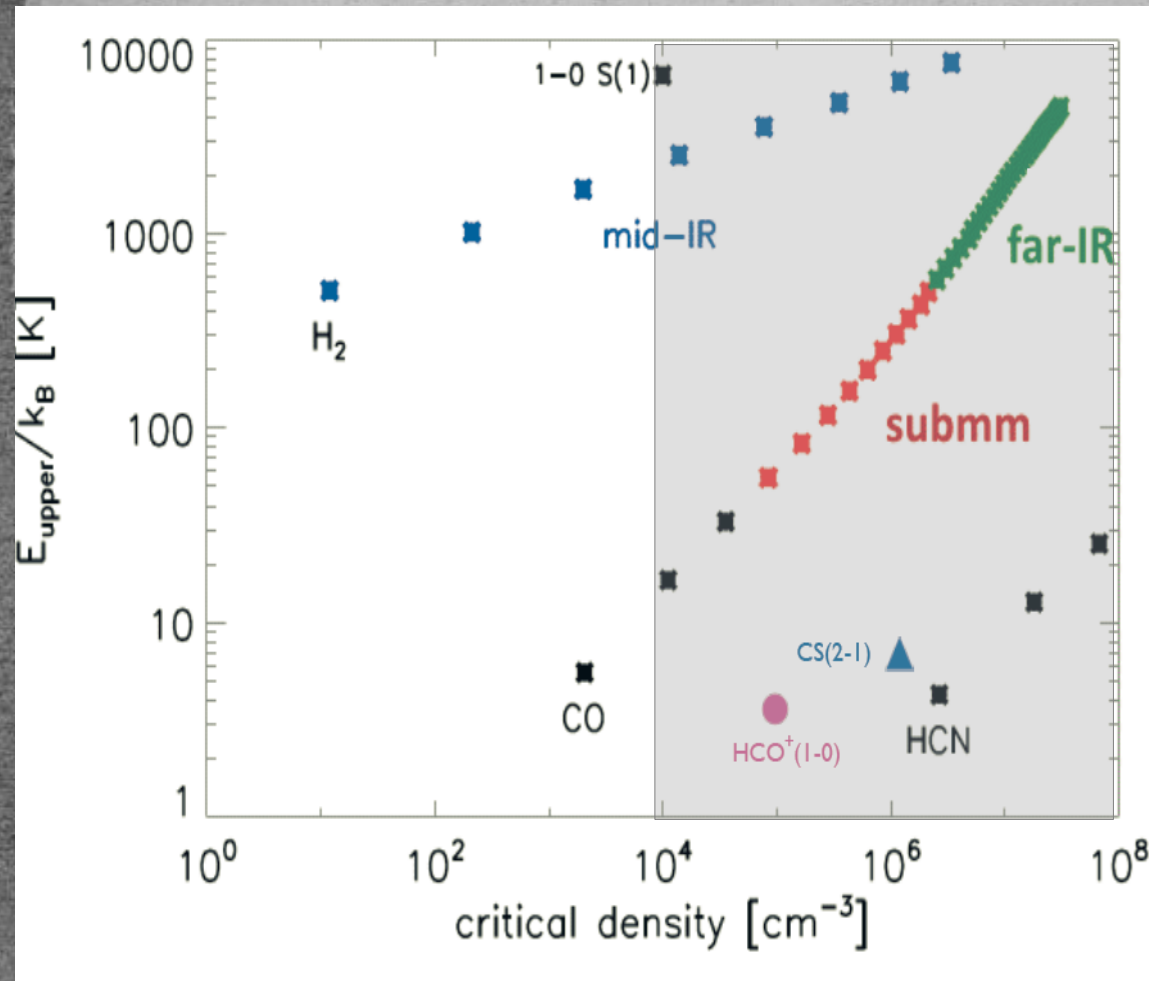
A step in the dark: The Dense Molecular Gas (DeMoGas) in Galaxies

Manolis Xilouris (ISAARS-NOA)

Zhi-Yu Zhang (IfA, University of Edinburgh / ESO)

Thomas R. Greve (UCL)

Molecular gas and ISM



H_2 : Dominant in molecular gas BUT difficult to be observed (small transition probabilities and relatively high-excitation levels)

Carbon monoxide (CO): the second most abundant molecule \rightarrow easily excited at low temperatures (e.g. $\sim 5\text{K}$ for the 1st excitation level)

Dense gas molecules: (such as HCN, HCO^+ , CS etc): have high-dipole moments thus high critical densities.

$$n_{\text{crit}} = A_{ul} / \sum(\Gamma_{u \neq l})$$

A_{ul} : Einstein coefficient for spontaneous emission

Γ : Collision rate coefficient

Importance of dense molecular gas: The gas that forms stars...

IR and millimeter studies of Giant Molecular Clouds (GMCs) in our Galaxy have shown that stars form in dense cores (e.g. Evans 1999, 2008; Wu et al 2010)

The dense gas residing in these cores is best traced by molecules with high critical densities.

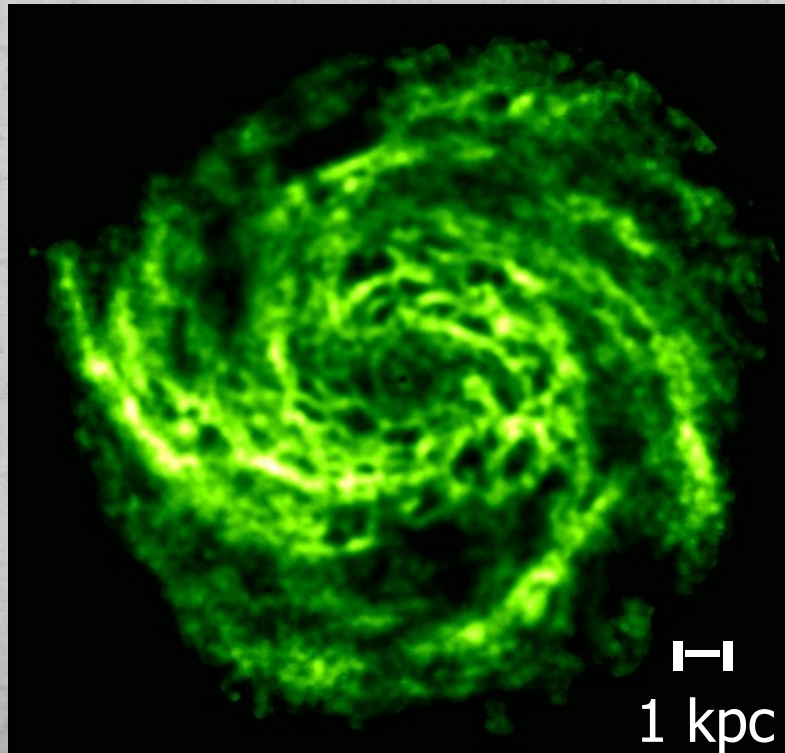
Importance of dense molecular gas: Which gas is forming stars?

IR and millimeter studies of Giant Molecular Clouds (GMCs) in our Galaxy have shown that stars form in dense cores (e.g. Evans 1999, 2008; Wu et al 2010)

The dense gas residing in these cores is best traced by molecules with high critical densities.

IC 342

HI (atomic gas)



THINGS

Importance of dense molecular gas: Which gas is forming stars?

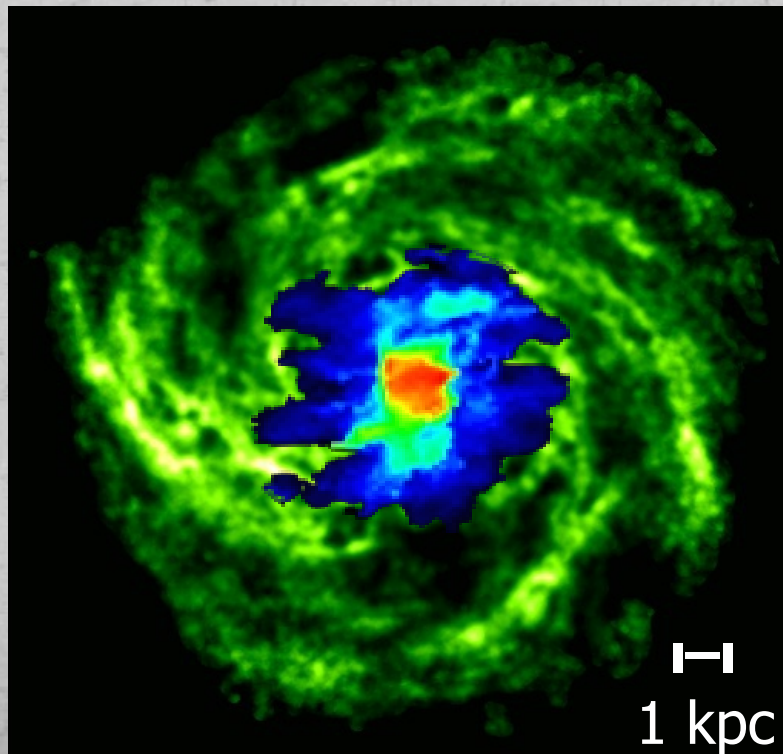
IR and millimeter studies of Giant Molecular Clouds (GMCs) in our Galaxy have shown that stars form in dense cores (e.g. Evans 1999, 2008; Wu et al 2010)

The dense gas residing in these cores is best traced by molecules with high critical densities.

IC 342

HI (atomic gas)

$^{12}\text{CO J=1-0}$
(molecular gas)



THINGS

NRAO 12m

Importance of dense molecular gas: Which gas is forming stars?

IR and millimeter studies of Giant Molecular Clouds (GMCs) in our Galaxy have shown that stars form in dense cores (e.g. Evans 1999, 2008; Wu et al 2010)

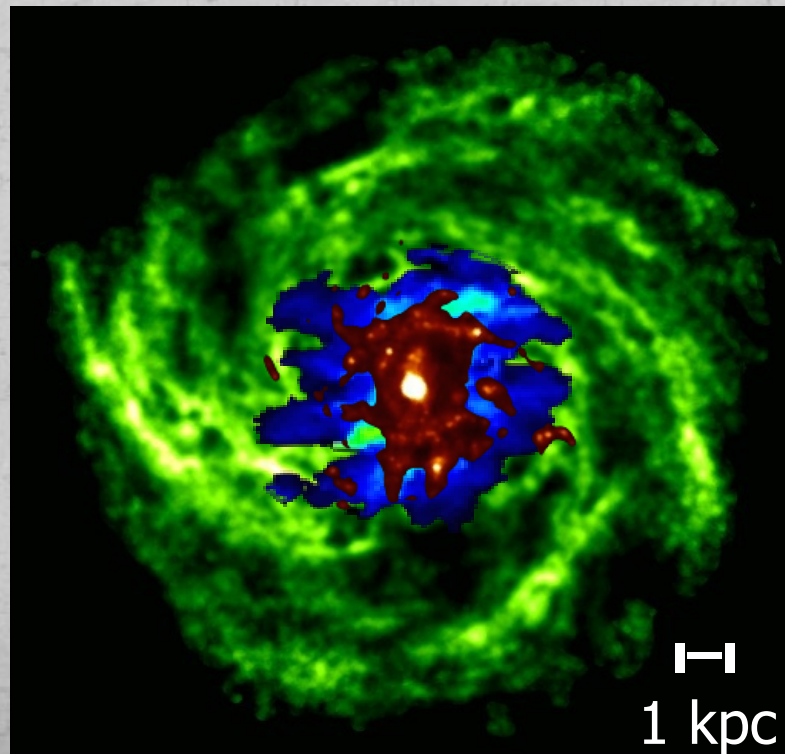
The dense gas residing in these cores is best traced by molecules with high critical densities.

IC 342

HI (atomic gas)

$^{12}\text{CO J=1-0}$
(molecular gas)

IR emission
(star formation)



THINGS

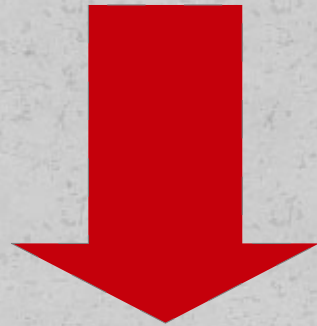
NRAO 12m

Spitzer 70um

Importance of dense molecular gas: Which gas is forming stars?

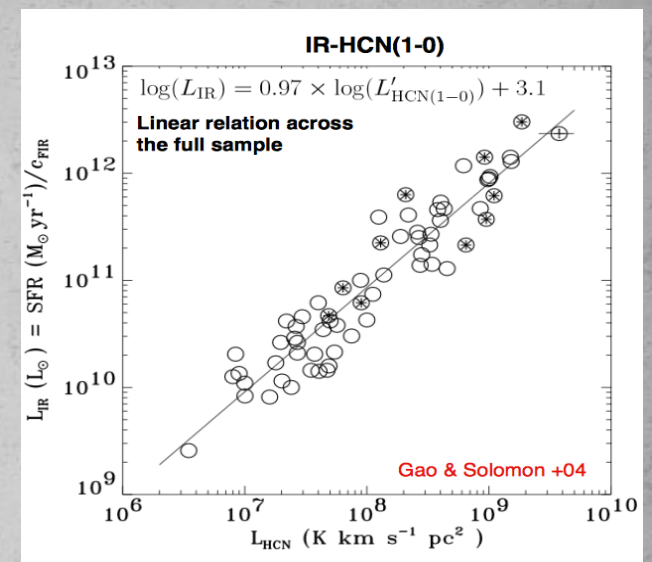
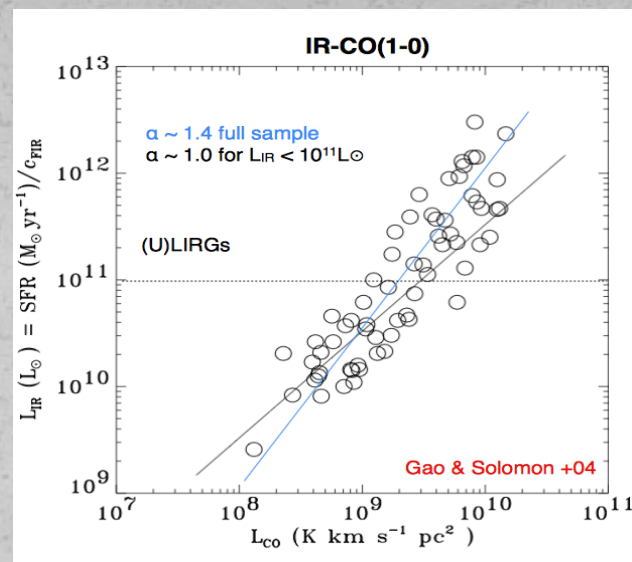
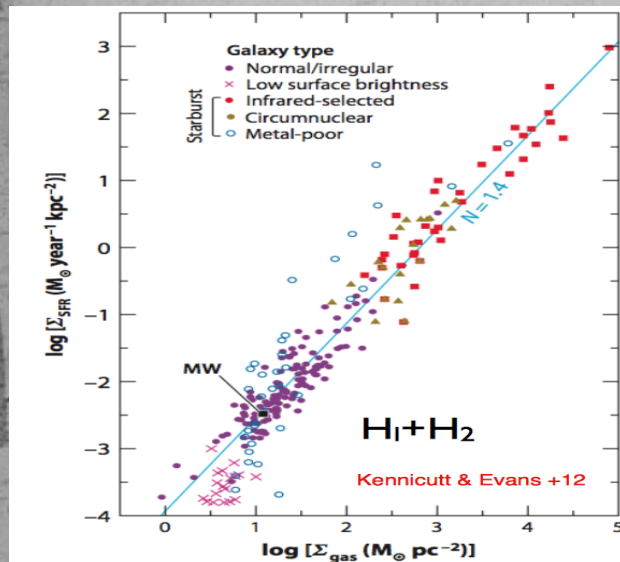
IR and millimeter studies of Giant Molecular Clouds (GMCs) in our Galaxy have shown that stars form in dense cores (e.g. Evans 1999, 2008; Wu et al 2010)

The dense gas residing in these cores is best traced by molecules with high critical densities.



Its presence and physical conditions correlate with SFR.

Star Formation laws in galaxies



ISSUES

- 'Mixing' populations
- CO-to- H_2 conversion factor (constant or varying?)
- Mixing J-transitions
- ...

Dense gas (traced by HCN, CS etc), not the total gas ($H_2 + HI$), is the key to star formation.

Challenges

- Are SF laws universal i.e. are the same for local/high- z galaxies or different types of galaxies (disks, starbursts)?
- Can we tie the observed SF laws to physical mechanisms governing/regulating star formation, and if so what are they?

Aim:

Probe the densest regions in galaxies (where star formation occurs) and derive the physical properties of the dense gas, *using well-sampled high- J CO SLEDs and/or multi- J observations of heavy rotor molecules.*

- The nature of the SF laws in the dense gas
- The heating mechanisms occurring within dense gas ($n_{\text{crit}} > 10^4 \text{ cm}^{-3}$)

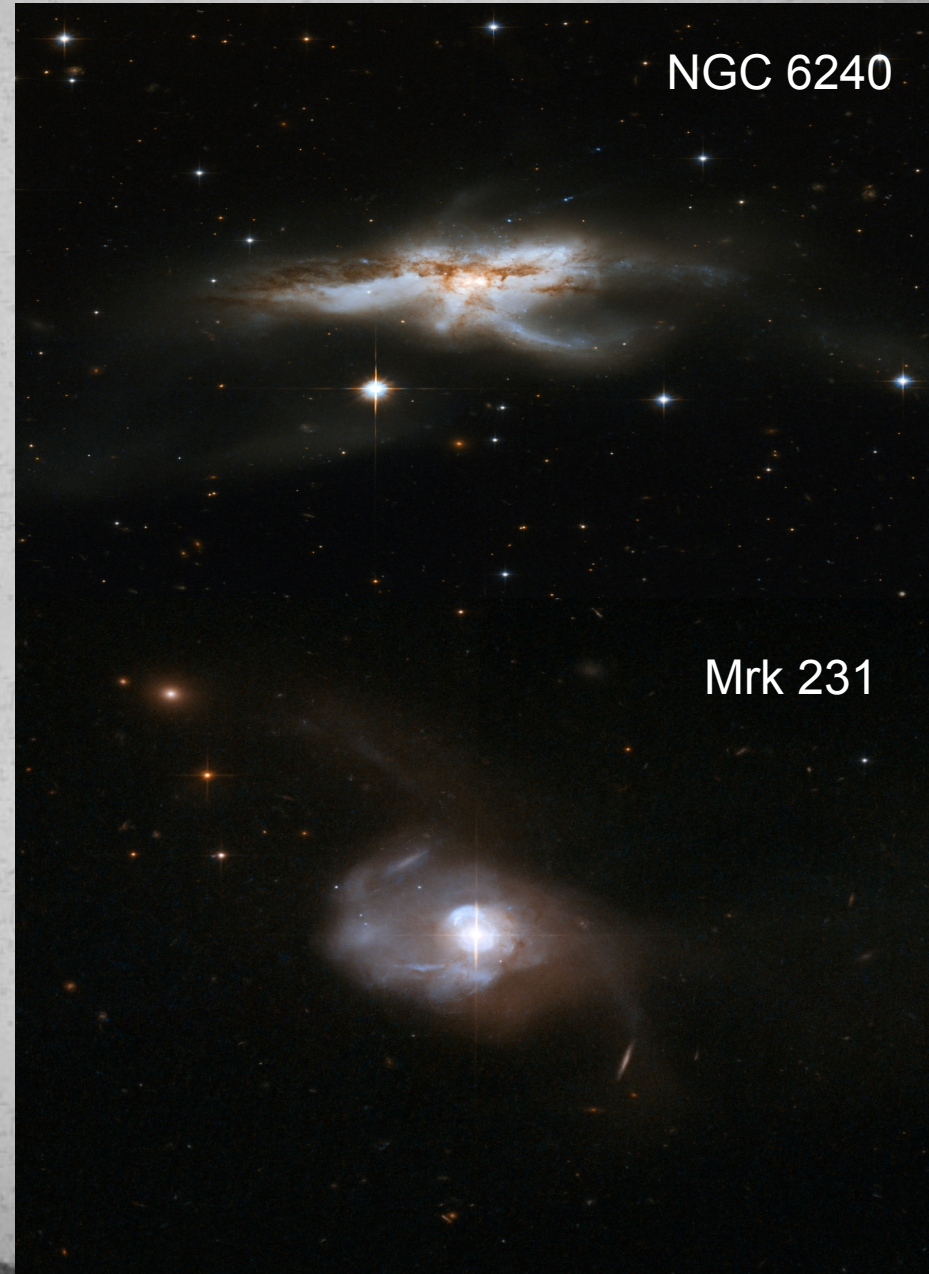
(Ultra) Luminous Infrared Galaxies

- Characteristic IR luminosity:

$$\text{LIRGs} \geq 10^{11} L_{\odot}$$

$$\text{ULIRGs} \geq 10^{12} L_{\odot}$$

- Most of their energy (90%-95%) is infrared
- Associated with interactions/mergers
- Mix of starbursts and AGNs
- Rich in molecular gas



HerCULES Sample

29 galaxies ($z < 0.1$) (all observed within the framework of the Herschel Comprehensive (U)LIRG Emission Survey, PI: van der Werf).

The galaxies were chosen from the IRAS BGS and fulfill the following criteria:

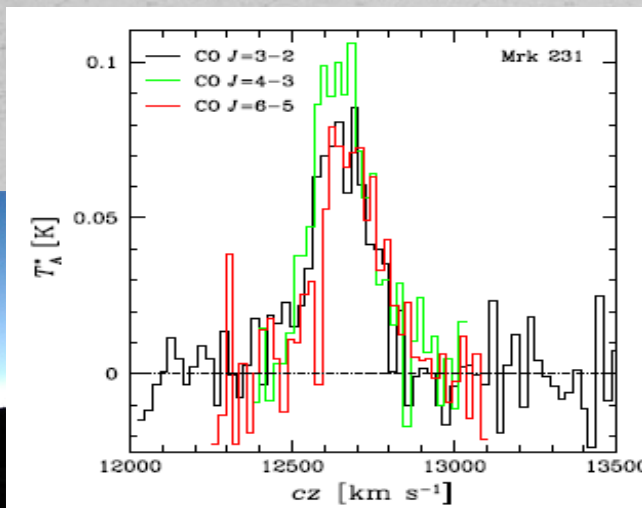
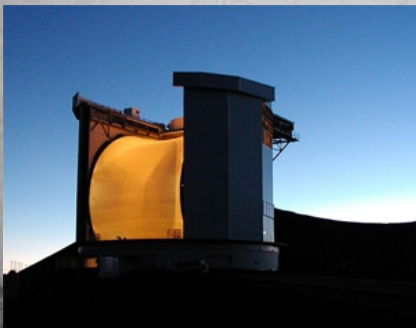
$$S_{60} > 11.65 \text{ Jy (LIRGs - } L_{\text{IR}} > 10^{11} L_{\odot})$$

$$S_{60} > 16.4 \text{ Jy (ULIRGs - } L_{\text{IR}} > 10^{12} L_{\odot})$$

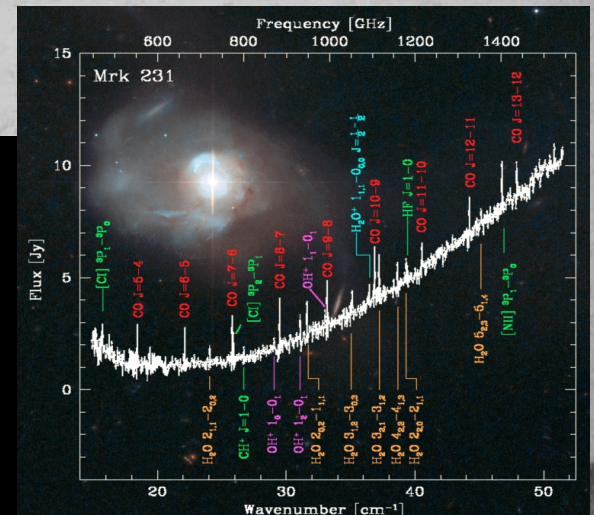
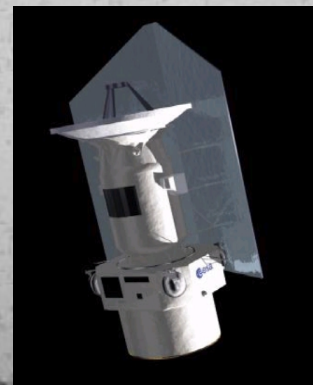
CO J=1-0 to J=4-3
(Papadopoulos et al. 2012)

CO J=5-4 up to J=13-12

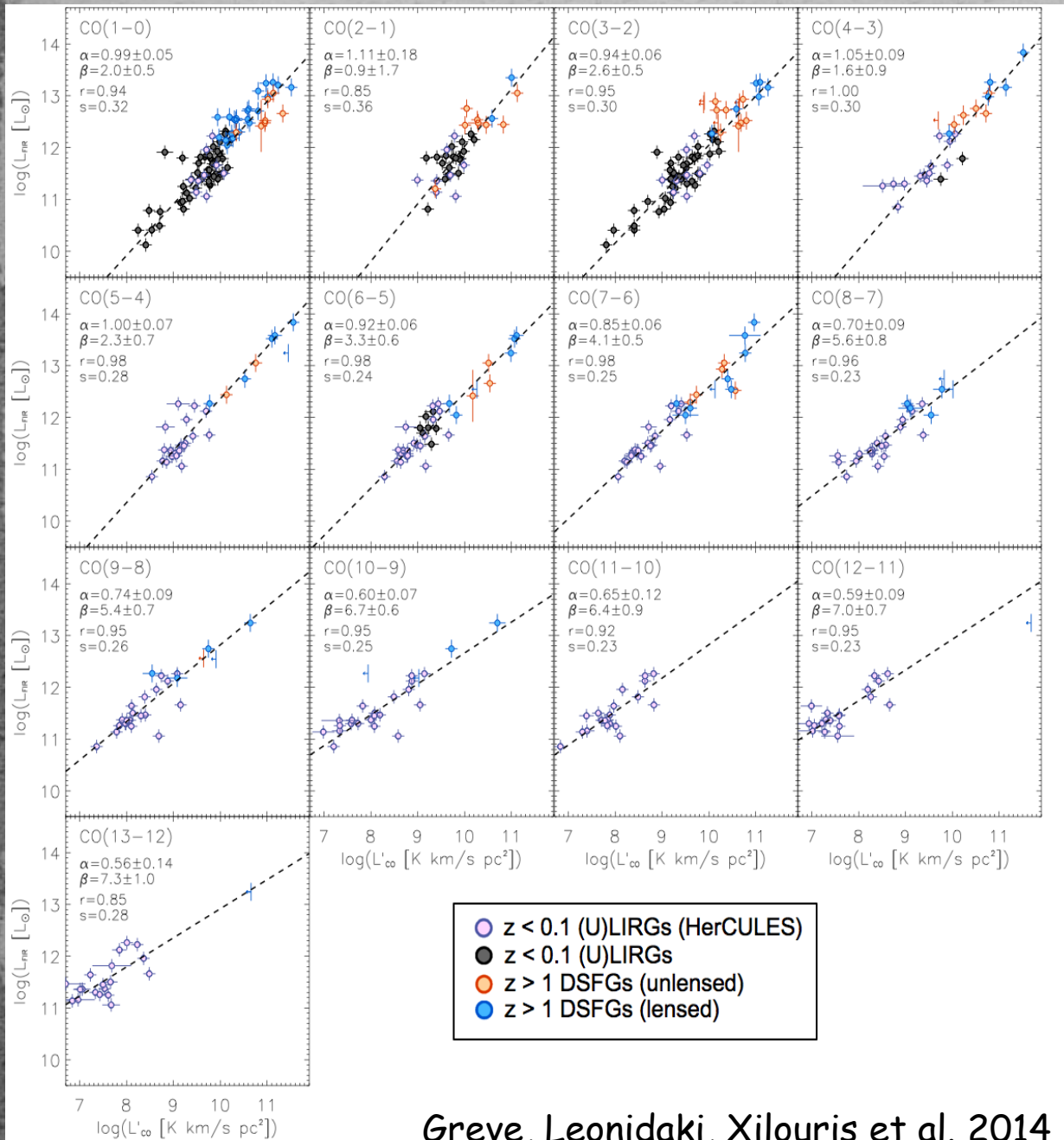
JCMT



HERSCHEL



Observing the CO ladder in local (U)LIRGs

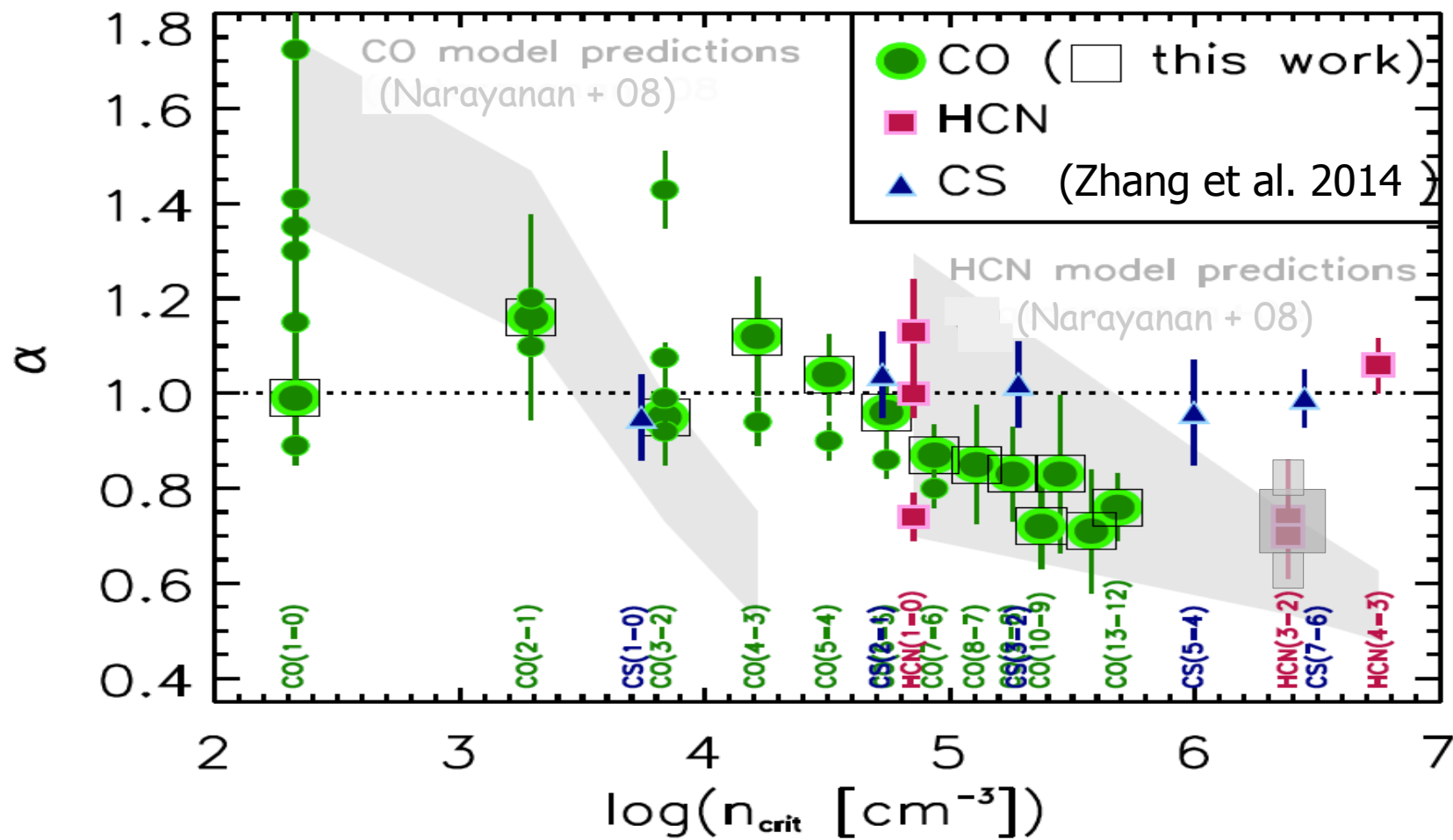


We study the SF laws for the entire CO rotational ladder up to $J=13-12$ for a large, well-defined sample of local (U)LIRGs as well as high- z dusty star forming galaxies (DSFGs)

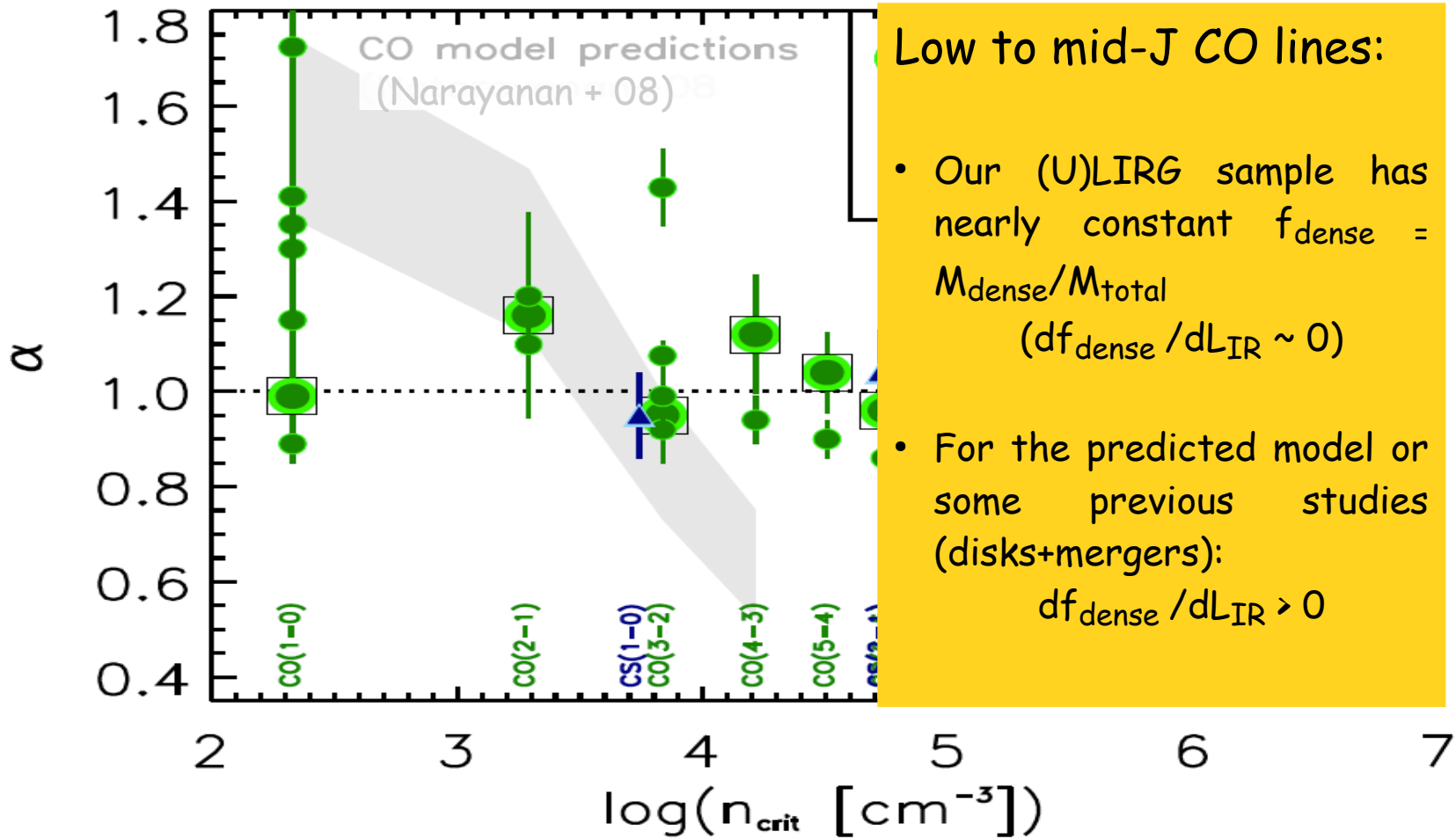
Functionals of the form
 $L_{\text{FIR}} = a L'_{\text{CO}} + \beta$
 were fitted to the data

- low- to mid- J CO transitions (up to $J=5-4$) - $\rightarrow a \sim 1$.
- CO $J=6-5$ and beyond - $\rightarrow a < 1$

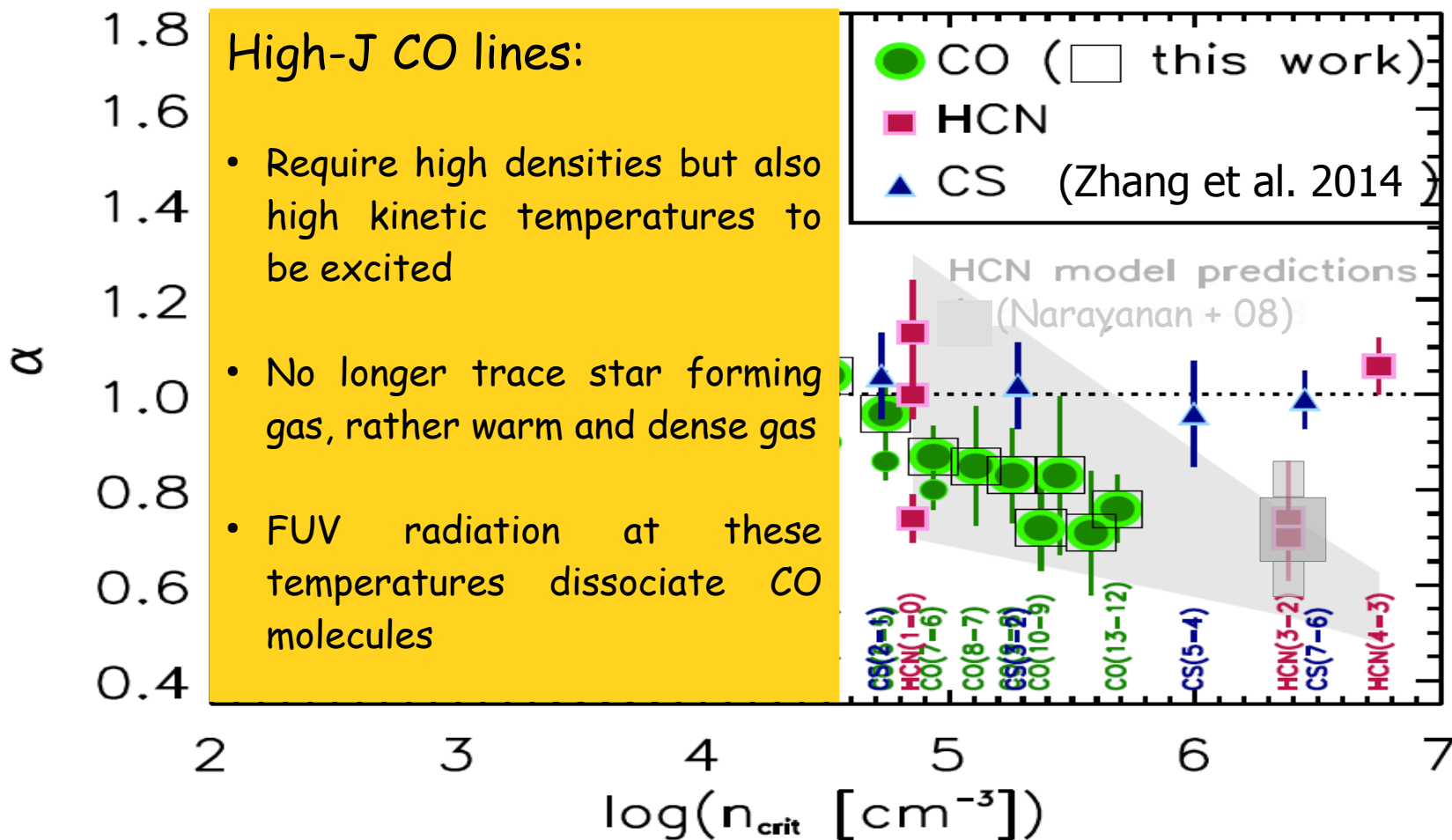
IR-mol slope vs. critical density



IR-mol slope vs. critical density



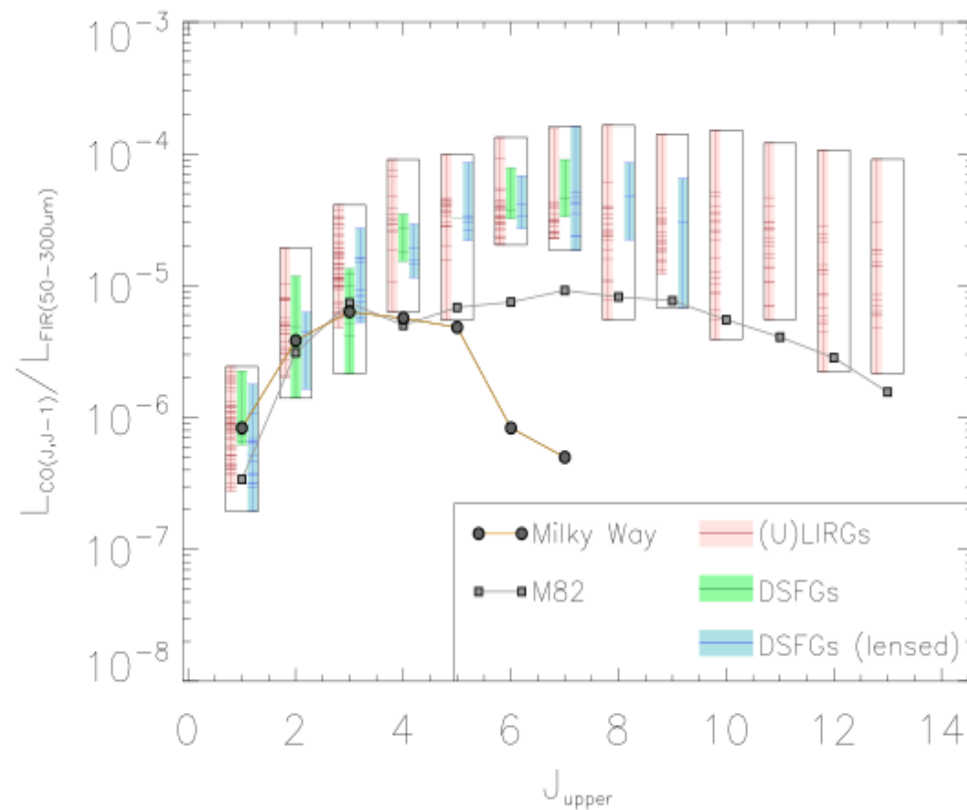
IR-mol slope vs. critical density



Evidence of a warm ($T_{\text{kin}} > 100\text{K}$) and dense ($n > 10^4 \text{cm}^{-3}$) gas phase:

- detached from the star formation
- Not tied to UV heating -> Suggestive of alternative heating mechanisms (cosmic rays, mechanical heating via SN turbulence/shocks)

A more direct indication of significant amounts of dense and warm gas in our (U)LIRG-dominated sample:



- Global CO SLEDs remain nearly flat out to $J=13-12$!
- Radically different from MW/quiescent CO SLEDs

* Under the program "A Step in the Dark: The Dense Molecular Gas (DeMoGas) in Galaxies" (<http://demogas.astro.noa.gr>)

Abstract:

We present IR – CO luminosity relations (i.e., $\log L_{\text{FIR}} = \alpha \log L'_{\text{CO}} + \beta$) across the CO rotational ladder (continuously from $J = 1 - 0$ to $J = 13 - 12$) for a sample of 87 (Ultra) Luminous Infra-red Galaxies observed either with Herschel SPIRE-FTS and/or with ground-based telescopes. To extend our analysis to high redshifts, we included 76 (sub-)millimeter selected dusty star forming galaxies from the literature with robust CO observations and well-sampled far-IR/sub-millimetre spectral energy distributions (SEDs). The derived FIR – CO luminosity relations are linear (i.e., slopes, α , consistent with unity) for $J=1-0$ to $J=5-4$ (corresponding to gas densities of $\sim 3 \times 10^2 - 4 \times 10^3 \text{ cm}^{-3}$), and become increasingly sub-linear ($\alpha < 1$) for the higher transitions. The latter is attributed to the higher α lines becoming sub-thermally excited, as seen in the turn-over at high- J in the CO SLEDs of our sources. We provide a simple theoretical framework with which to understand the observed trends.

Galaxy samples & Data:

Low-z samples:

* 70 local (U)LIRGs at $z < 0.1$ selected from the IRAS BGS ($f_{60\mu\text{m}} > 5.24 \text{ Jy}$). The IR/submm data for this sample were culled from a number of studies (see Papadopoulos et al. (2012) and references therein). The CO line data consisted of new ground-based, single-dish observations of CO $J=1-0$ to 4-3, and $J=6-5$ for subsets of the full sample, augmented by an exhaustive compilation of literature measurements.

* To extend our study to the highest CO transitions, we included data from the Herschel Comprehensive (U)LIRG Emission Survey (HerCULES; van der Werf et al. (2010)) – an open time key program on the ESA Herschel Space Observatory (Pilbratt et al. 2010) which measured CO $J=4-3$ to $J=13-12$ for 29 local (U)LIRGs using the Fourier-transform spectrograph (FTS) of the SPIRE instrument (Griffin et al. 2010).

High-z samples:

* Dusty star forming galaxies (DSFGs), selected at (sub-)millimetre wavelengths, are thought to harbour the same extreme ISM and star forming conditions as local (U)LIRGs, and were for that reason chosen as our high-z comparison sample. As for the local (U)LIRGs, we carefully sifted through the literature and NED archives from that compiled an exhaustive data-base of all CO line measurements of DSFGs at $z > 1$, as well as of their optical/UV/near-IR and far-IR/(sub)mm/radio continuum data (see Greve, in prep. for details). A total of 76 DSFGs were found. However, only 49 DSFGs went in to our final analysis, as only these sources had sufficient far-IR/submm continuum measurements that reliable estimates of the IR luminosities could be made (see below). Of these 49 sources, 25 were strongly lensed DSFGs (e.g., The Eyzies; Swinbank et al. (2010)). In total, our analysis is based on 117 CO detections towards 49 DSFGs.

SED fitting and L_{FIR} estimates

* The pan-chromatic (from far-UV/optical to radio) spectral energy distributions (SEDs) of our sample galaxies were modeled using CIGALE (Code Investigating GALaxy Emission – Burgarella et al. (2005); Noll et al. (2009)). CIGALE employs dust-attenuated stellar population models to fit the far-UV/optical SED, while at the same time ensuring that the dust-absorbed UV photons are re-emitted in the far-IR, thus ensuring energy-balance between the far-UV and far-IR. The far-IR/submm continuum is modeled using the templates by Dale & Helou (2002) and Chary & Elbaz (2001).

* Excellent fits were obtained for all of the local galaxies due to their well-sampled SEDs. For the high-z galaxies, only sources with data points longward and shortward of (or near) the expected dust peak were included in the final analysis (49 sources). All SED fits used in this paper can be found at <http://demogas.astro.noa.gr>. From the SED fits we derived the far-IR (L_{FIR} , from 50 to 300 μm) luminosity. The accuracy of our IR/far-IR luminosity estimates were estimated as the $1-\sigma$ dispersion of the distributions obtained through bootstrapping of the photometry errors 1000 times.

Fig.2: Slope (α) determinations

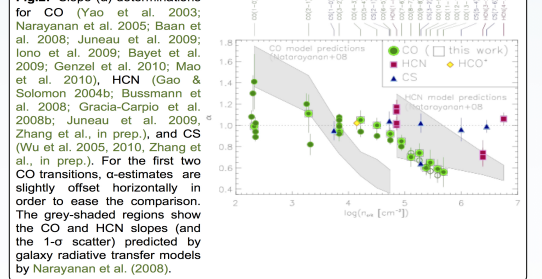
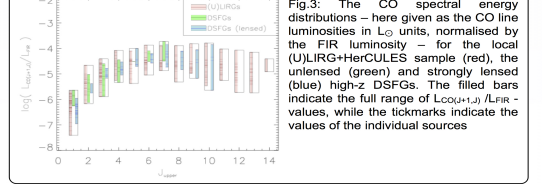


Fig.3: The CO spectral energy distributions



A more direct ir
(U)LIRG-dominant

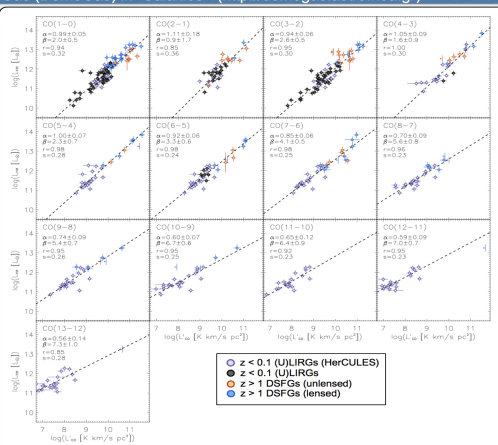
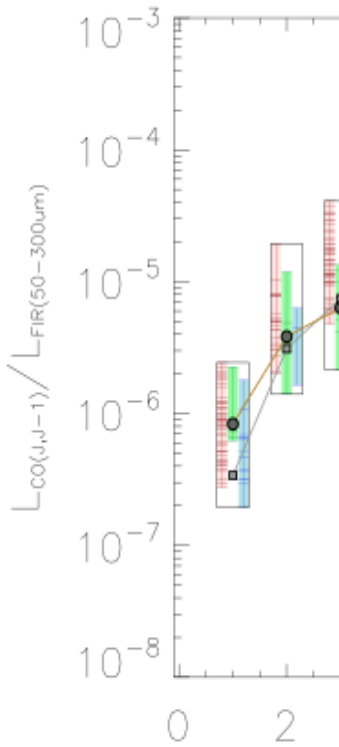


Fig.1: $\log L_{\text{FIR}}$ vs. $\log L'_{\text{CO}}$ across the CO rotational ladder (from $J=1-0$ to $J=13-12$). The low- z ($z < 0.1$) data include the (U)LIRG sample from Papadopoulos et al. (2012) (dark-grey symbols) with CO observations from $J=1-0$ to $J=6-5$, and (U)LIRGs from HerCULES (van der Werf et al. (2010)) (pink symbols). The high- z ($z > 1$) sources are unlensed, or weakly lensed, DSFGs (yellow symbols) and strongly lensed DSFG (blue symbols) uncovered from various (sub)millimetre surveys. The dashed lines show the best fits of the functional $\log L_{\text{FIR}} = \alpha \log L'_{\text{CO}} + \beta$ to the data, with the optimum parameter (α , β) values and their errors indicated in each panel. The scatter (s) of the data around the best fits along with the correlation coefficient (r) are given in each panel.

Analysis & Discussion

* The FIR-CO relations derived here are shown in Fig. 1. This is the first time that FIR-CO relations have been directly inferred from observations up to such high J -transitions. Statistically significant correlations are seen across the board and functionals of the form $L_{\text{FIR}} = \alpha L'_{\text{CO}} + \beta$ were fitted to the data (dashed lines in Fig.1)

* For the low- to mid- J CO transitions (up to $J=5-4$) we find FIR-CO slopes of unity. This is in agreement with some previous studies, although super-linear slopes have also been found and are in fact predicted by models (Krumholz & Thompson 2007; Narayanan et al. 2008). See Fig. 2. A slope of 1.5 is expected for CO transitions that trace the bulk of the star forming ISM in galaxies, provided that a fixed fraction of the gas mass ($M_{\text{gas}} - p$) is turned into stars every free-fall time ($t_{\text{ff}} - p^{-0.5}$).

* For CO transitions $J=6-5$ and beyond we find statistically significant sub-linear FIR-CO slopes, with the slopes becoming shallower with increasing J (Fig. 2). The sub-linear slopes are explained by the fact that the high- J CO lines not only require high densities but also high kinetic temperatures to be excited. In fact, from Fig. 3 we see that the lines become significantly sub-thermal, meaning that the lines no longer trace the star forming gas. Although, the models qualitatively agree with these findings, the predicted sub-linearity sets in at much lower transitions ($J=3-2$) than what is observed.

* Finally, we note that for the true high density gas tracers like HCN and CS, the observations strongly favour linear slopes (cf. Bussmann et al. 2008; Juneau et al. 2009).

* All of the above findings can be explained by a simple theoretical argument, inspired by that of Wilson & Blitz (2002). Consider that for a given CO transition, $\alpha = \text{dlog}(L_{\text{FIR}})/\text{dlog}(L'_{\text{CO}})$ can be expressed as:

$$\alpha = \frac{d \log L_{\text{FIR}}}{d \log L_{\text{HCN}}} \times \frac{d \log L_{\text{HCN}}}{d \log L'_{\text{CO}}} = \alpha_{\text{dense}} \left(1 + \frac{d \log f_{\text{dense}}}{d \log L'_{\text{CO}}} \right)$$

where α_{dense} is the slope of the FIR-HCN(1-0) relation which has been shown to be unity ($\alpha_{\text{dense}} = 1.00 \pm 0.05$; Gao & Solomon 2004). f_{dense} is a measure of the cold, dense gas fraction, i.e. the gas phase that is actively forming stars. There are two cases to consider:

Low- to mid- J CO lines: will trace the bulk of the star forming gas, and we therefore expect f_{dense} to increase or stay a minimum stay constant with increasing L'_{CO} , thus rendering $\alpha \geq 1$. Since we are considering similar galaxy populations (ULIRGs and DSFGs), with not too dissimilar f_{dense} , the second term in the parenthesis vanishes, and we would thus expect α -values of roughly unity, as observed.

High- J lines: the CO lines no longer trace the star forming gas, but rather hot gas. As L'_{CO} increases we may therefore no longer expect f_{dense} to increase; rather we expect the opposite, i.e. implying a negative $\text{dlog}(f_{\text{dense}}) - \text{dlog}(L'_{\text{CO}})$ gradient, and thus $\alpha < 1$.

nd warm gas in our

CO SLEDs remain
at out to $J=13-12$!

different from
scent CO SLEDs

Tracing star formation relations across the CO ladder and redshift space*

Manolis Xilouris¹, Ioanna Leonidak¹, Thomas R. Greve², Zhi-Yu Zhang³

1. National Observatory of Athens – IAASARS, Greece

2. Department of Physics and Astronomy, University College London, UK

3. European Southern Observatory, Garching, Germany

* Under the program "A Step in the Dark: The Dense Molecular Gas (DeMoGas) in Galaxies" (<http://demogas.astro.noa.gr>)

Abstract:

We present IR – CO luminosity relations (i.e., $\log L_{\text{FIR}} = \alpha \log L'_{\text{CO}} + \beta$) across the CO rotational ladder (continuously from $J = 1 - 0$ to $J = 13 - 12$) for a sample of 87 (Ultra) Luminous Infra-red Galaxies observed either with Herschel SPIRE-FTS and/or with ground-based telescopes. To extend our analysis to high redshifts, we included 76 (sub)-millimeter selected dusty star forming galaxies from the literature with robust CO observations and well-sampled far-IR/sub-millimetre spectral energy distributions (SEDs). The derived FIR – CO luminosity relations are linear (i.e. slopes, α , consistent with unity) for $J=1-0$ to $J=4-3$ (corresponding to gas densities of $\sim 3 \times 10^2 - 4 \times 10^3 \text{ cm}^{-3}$), and become increasingly sub-linear ($\alpha < 1$) for the higher transitions. The latter is attributed to the higher- J lines becoming sub-thermally excited, as seen in the turn-over at high- J in the CO SLEDs of our sources. We provide a simple theoretical framework with which to understand the observed trends.

Galaxy samples & Data:

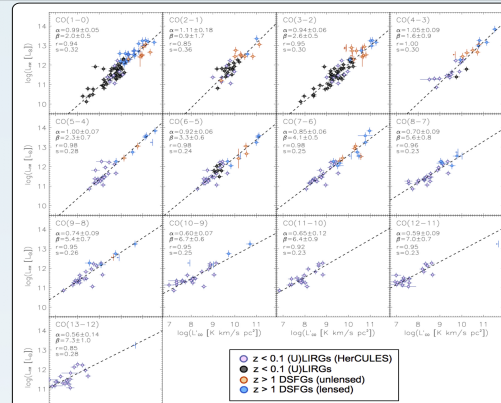
Low-z samples:

* 70 local (U)LIRGs at $z < 0.1$ selected from the IRAS BGS ($f_{60\mu\text{m}} > 5.24 \text{ Jy}$). The IR/submm data for this sample were culled from a number of studies (see Papadopoulos et al. (2012) and references therein). The CO line data consisted of new ground-based, single-dish observations of CO $J=1-0$ to $J=6-5$ for subsets of the full sample, augmented by an exhaustive compilation of literature measurements.

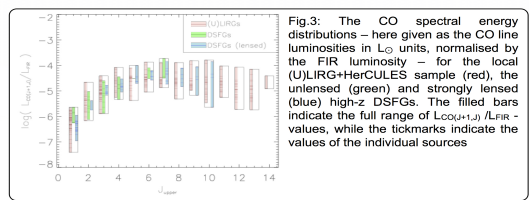
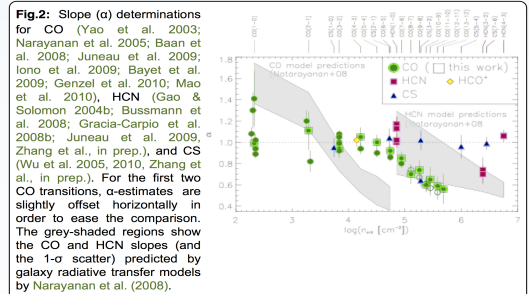
* To extend our study to the highest CO transitions, we included data from the Herschel Comprehensive (U)LIRG Emission Survey (HerCULES; van der Werf et al. (2010) – an open time key program on the ESA Herschel Space Observatory (Pilbratt et al. 2010) which measured CO $J=4-3$ to $J=13-12$ for 29 local (U)LIRGs using the Fourier-transform spectrophotograph (FTS) of the SPIRE instrument (Griffith et al. 2010).

High-z samples:

* Dusty star forming galaxies (DSFGs), selected at (sub)-millimetre wavelengths, are thought to harbour the same extreme ISM and star forming conditions as local (U)LIRGs, and were for that reason chosen as our high-z comparison sample. As for the local



estimates were estimated as the 1- σ dispersion of the distributions obtained through bootstrapping of the photometry errors 1000 times.



found and are in fact predicted by models (Krumholz & Thompson 2007; Narayanan et al. 2008). See Fig. 2. A slope of 1.5 is expected for CO transitions that trace the bulk of the star forming ISM in galaxies, provided that a fixed fraction of the gas mass ($M_{\text{gas}} - p$) is turned into stars every free-fall time ($t_{\text{ff}} - p^{-0.5}$).

* For CO transitions $J=6-5$ and beyond we find statistically significant sub-linear FIR-CO slopes, with the slopes becoming shallower with increasing J (Fig. 2). The sub-linear slopes are explained by the fact that the high- J CO lines not only require high densities but also high kinetic temperatures to be excited. In fact, from Fig. 3 we see that the lines become significantly sub-thermal, meaning that the lines no longer trace the star forming gas. Although, the models qualitatively agree with these findings, the predicted sub-linearity sets in at much lower transitions ($J=3-2$) than what is observed.

* Finally, we note that for the true high density gas tracers like HCN and CS, the observations strongly favour linear slopes (cf. Bussmann et al. 2008; Juneau et al. 2009).

* All of the above findings can be explained by a simple theoretical argument, inspired by that of Wong & Blitz (2002). Consider that for a given CO transition, $\alpha = d \log(L_{\text{FIR}}) / d \log(L'_{\text{CO}})$ can be expressed as:

$$\alpha = \frac{d \log L_{\text{FIR}}}{d \log L'_{\text{HCN}}} \times \frac{d \log L'_{\text{HCN}}}{d \log L'_{\text{CO}}} = \alpha_{\text{dense}} \left(1 + \frac{d \log f_{\text{dense}}}{d \log L'_{\text{CO}}} \right)$$

where α_{dense} is the slope of the FIR-HCN(1-0) relation which has been shown to be unity ($\alpha_{\text{dense}} = 1.00 \pm 0.05$; Gao & Solomon 2004). f_{dense} is a measure of the cold, dense gas fraction, i.e. the gas phase that is actively forming stars. There are two cases to consider:

Low- to mid-J CO lines: will trace the bulk of the star forming gas, and we therefore expect f_{dense} to increase or as a minimum stay constant with increasing L'_{CO} , thus rendering $\alpha \geq 1$. Since we are considering similar galaxy populations (ULIRGs and DSFGs), with not too dissimilar f_{dense} , the second term in the parenthesis vanishes, and we would thus expect α values of roughly unity, as observed.

High-J lines: the CO lines no longer trace the star forming gas, but rather hot gas. As L'_{CO} increases we may therefore no longer expect f_{dense} to increase; rather we expect the opposite, i.e. implying a negative $\log(f_{\text{dense}}) - \log(L'_{\text{CO}})$ gradient, and thus $\alpha < 1$.



Acknowledgements: the project "DeMoGas" is implemented under the "ARISTEIA" Action of the "OPERATIONAL PROGRAMME EDUCATION AND LIFELONG LEARNING", co-funded by the European Social Fund (ESF) and National Resources. References: Bayet et al. MNRAS, 299, 264 (2009); Dale & Helou ApJ, 556, 159 (2002); Gao & Solomon ApJS, 152, 63 (2004); Krumholz & Thompson ApJ, 669, 289; Narayanan et al. ApJ, 630, 269 (2008); Papadopoulos et al. MNRAS, 426, 2801 (2012).

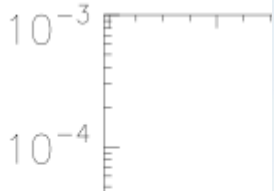
A more direct in (U)LIRG-dominant

and warm gas in our

A detailed analysis of the CO SLEDs, in conjunction with the multi-J HCN, CS and HCO⁺ line data-sets available for many of the (U)LIRGs, is needed !!

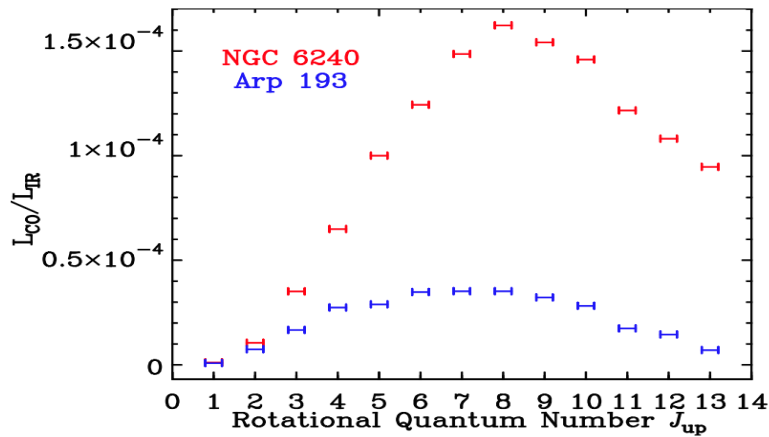
CO SLEDs remain

ascent CO SLEDs

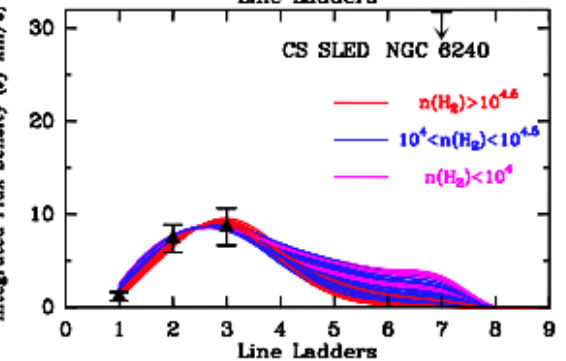
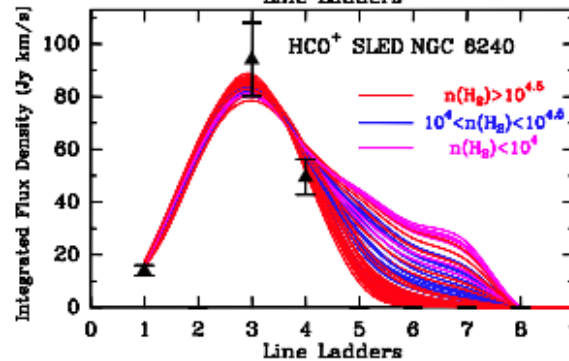
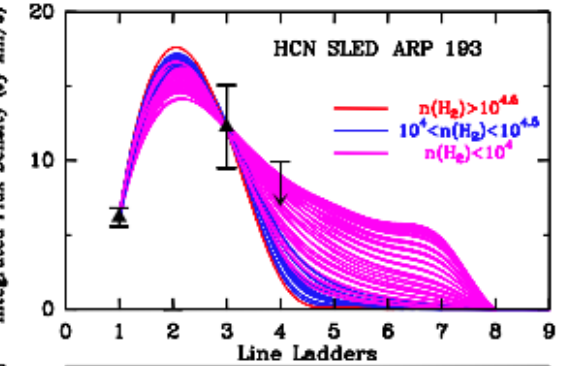
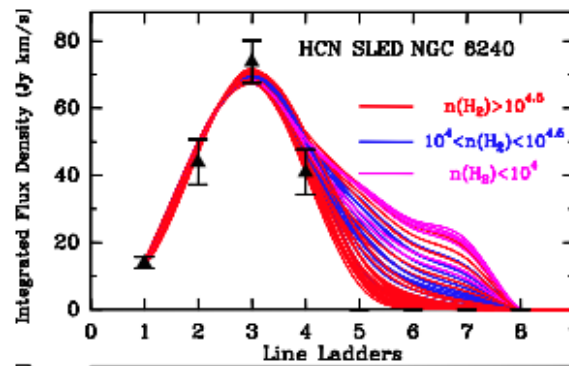
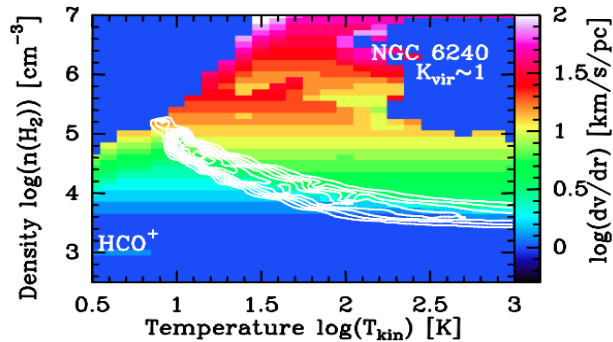
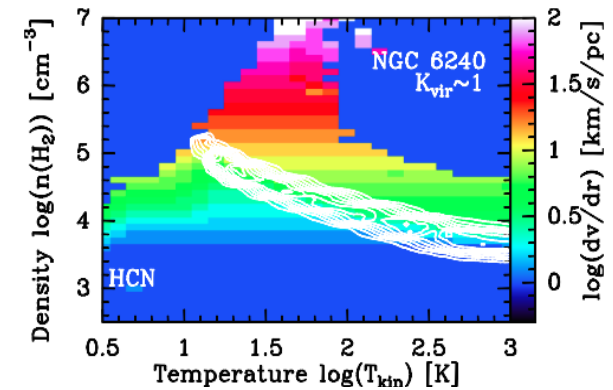


NGC 6240 and Arp 193 as case studies

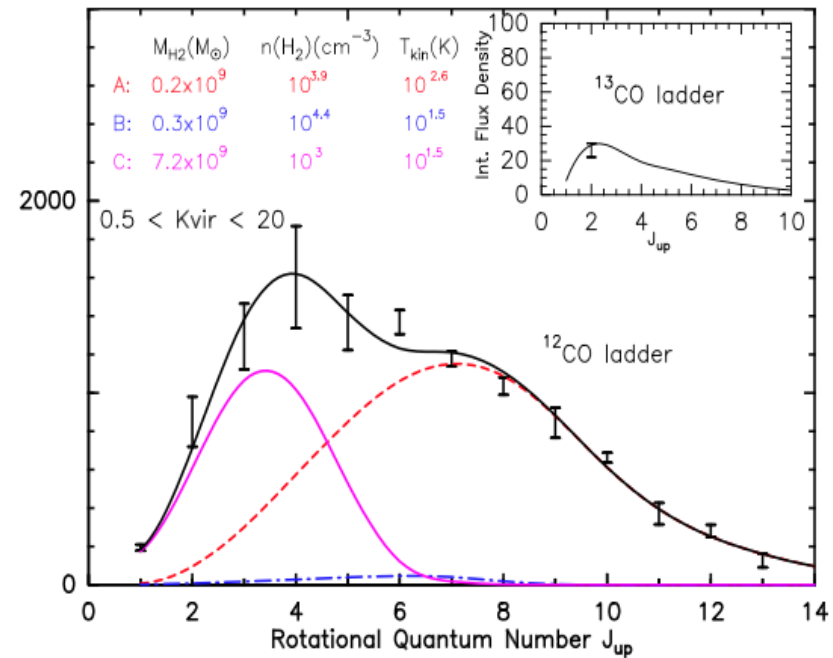
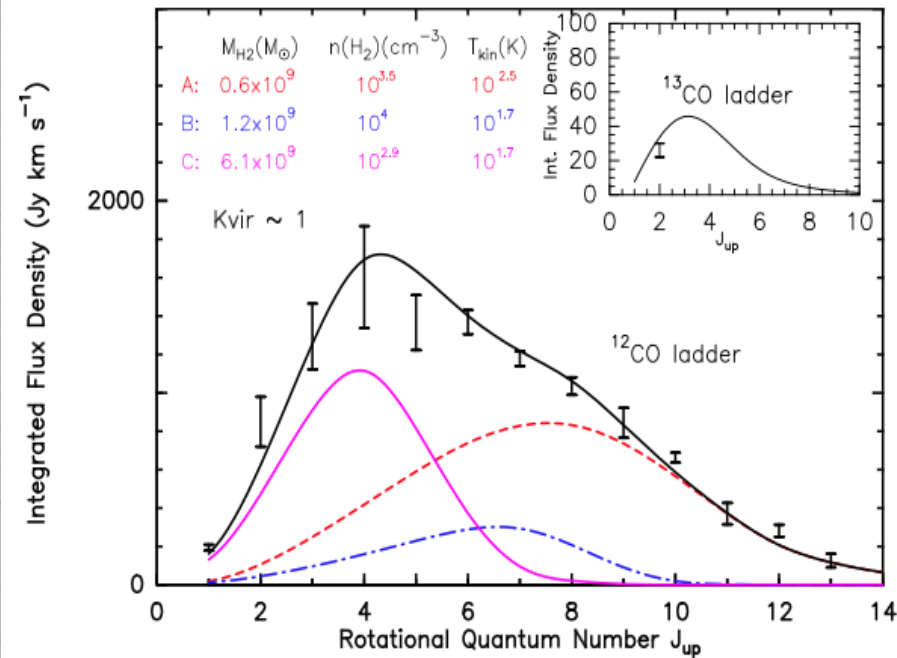
(Papadopoulos, Zhang, Xilouris et al. 2014)



The two CO SLEDs strongly diverge from J=4-3 onwards, with NGC 6240 having a much higher CO line excitation than Arp 193, despite their similar low-J CO SLEDs



NGC6240 and Arp193 as case studies (Papadopoulos, Zhang, Xilouris et al. 2014)



The two CO SLEDs for Arp193. The dense components (red, blue dotted lines) are drawn from LVG solution space compatible with the HCN SLED of this system while the pink line shows a lower-density and lower-temperature component, which accounts for most of the gas mass.

Rest of the HeRCULEs sample...

In hand a representative flux-limited sample of local LIRGs and (U)LIRGs (HeRCULES sample) with:

- Comprehensive coverage of the entire CO ladder (from J=1-0 up to J=13-12)
- All available molecular spectral lines that are good dense gas tracers (e.g. CS, HCN, HCO⁺, HNC, CN).

Sample

Complete census of the molecular Interstellar Medium (ISM) to date in a large, homogeneous sample of local (U)LIRGs.

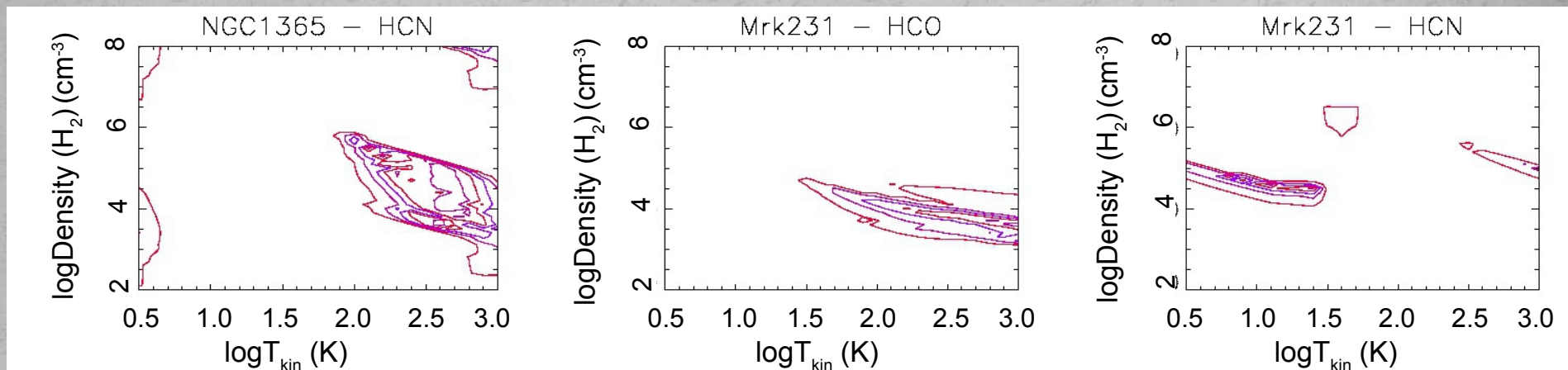
flux-limited sample of local LIRGs and (from J=1-0 up to J=13-12)

- All available molecular species (e.g. CS, HCN, HCO⁺, HNC, CN).

Table 11. NGC 7469 (IRAS 23007+0836, Mrk 1514)

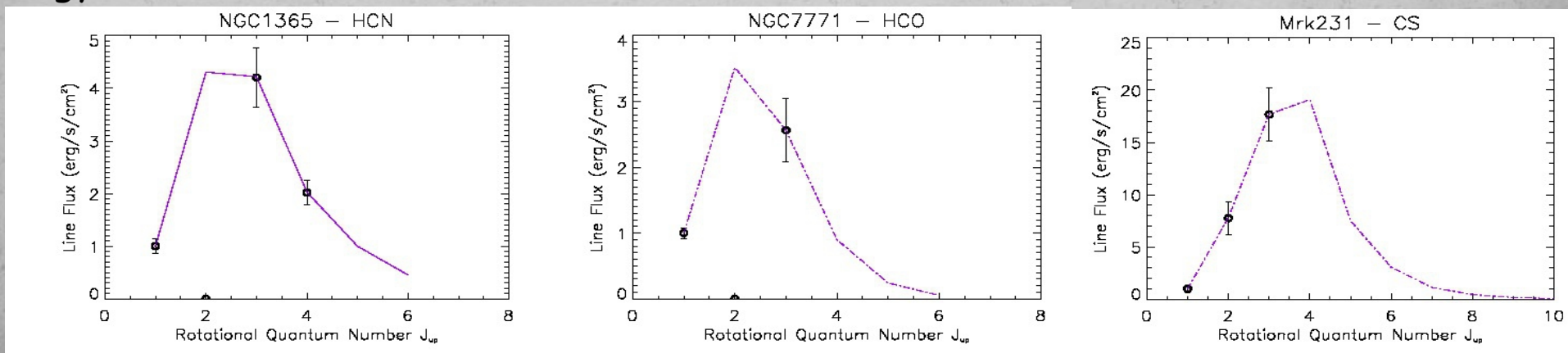
Line	Telescope	ν_{rest} (GHz)	θ_b ($''$)	$\frac{k_b}{A_p} \left(\frac{A_p 42''}{A_p 42''} \times \frac{F_{42''}}{F_{42''}} \right)$	Flux (Jy km/s)	Flux _{bc} (Jy km/s)	Ref
CS(2-1)	IRAM-30m	97.980	26 ¹	$\times 0.994769$	3.54 ± 0.6		ZY
	IRAM-30m		26 ¹	$\times 0.994769$	5.9 ± 0.59		ZY
	IRAM-30m		26 ¹	$\times 0.994769$	4.1 ± 0.7		IRAM30m-077-12
CS(3-2)	IRAM-30	146.969	17 ¹	$\times 0.986248$	5.76 ± 0.6		ZY
CS(5-4)	IRAM-30	244.935	10 ¹	$\times 0.966732$	4.74 ± 1.6		ZY
CS(7-6)	APEX	342.883	18	$\times 0.98762$	≤ 56.2		ZY14
HCO ⁺ (1-0)	IRAM-30m	89.188	29	$\times 0.996351$	13.2 ± 0.59		C11
	IRAM-30m		28	$\times 0.995886$	16.2 ± 0.6		GC08
HCO ⁺ (3-2)	IRAM-30m	267.557	9	$\times 0.961105$	19.8 ± 4		GC08
HCO ⁺ (4-3)	APEX	356.734	18	$\times 0.98762$	53.36 ± 10.7		ZY14
HCN(1-0)	IRAM-30m	88.63	28 (90 GHz)	$\times 0.995886$	11.1 ± 0.54		GC08
	OSO		44 (89 GHz)	$\times 1$	30.22 ± 6.04		P-B07(Curran et al. 2000)
	IRAM-30m		29	$\times 0.996351$	11.8 ± 0.6		C11
	NRAO-12m		72	$\times 1$	10.5 ± 2.03		GSD4a
	NRAO-12m		63 (3mm)	$\times 1$	≤ 2.905		HB93
HCN(3-2)	IRAM-30m	265.886	9 (260 GHz)	$\times 0.961105$	24.84 ± 3.1		GC08
	SMT		30	$\times 0.996724$	19.5 ± 4.8		Bus08
HCN(4-3)	APEX	354.505	18	$\times 0.98762$	≤ 48		ZY14
CN(1-0)	OSO	113.387	34	$\times 0.997892$	21.6 ± 2.7		A02
HNC(1-0)	OSO	90.663	42	$\times 1$	21.7 ± 3.1		A02
	IRAM-30m		29	$\times 0.996351$	$6.48 \pm$		C11

- We have embarked on radiative transfer modeling for the HeRCULES sample, using the LVG code RADEX (van der Tak et al. 2007) in order to map a wide parameter space [$n(\text{H}_2)$, T_{kin} , $dv/dr/\text{abundance}$].



Probability density functions (pdfs) for NGC 1365 and Mrk231, as constrained by various heavy rotor lines (e.g. HCO^+ , HCN).

- The best LVG solution ranges are analyzed \rightarrow construction of their Spectral Line Energy Distributions (SLEDs).



Leonidaki et al., in preparation

FUTURE PLAN

- These will be matched with the complete CO SLEDs of the galaxies from J=1-0 to J=13-12, combining multiple molecules and multiple excitation components where necessary.

This way:

- ✓ it is possible to disentangle different molecular gas phases and possibly different molecular gas heating mechanisms.
- ✓ It will break the degeneracy between different parameters and will probe molecular gas physical conditions ranging from the cold and low-density average states in giant molecular clouds all the way up to the state of the gas found only near their star-forming regions